Hindawi Publishing Corporation
Advances in Electronics
Volume 2014, Article ID 246769, 12 pages
http://dx.doi.org/10.1155/2014/246769

Review Article

InAs/GaSb Type-II Superlattice Detectors

Elena A. Plis[1,2]

[1] *Center for High Technology Materials, Department of Electrical and Computer Engineering, University of New Mexico, Albuquerque, NM, USA*

[2] *Skinfrared, LLC, Lobo Venture Lab 801, University Boulevard, Suite 10, Albuquerque, NM 87106, USA*

Correspondence should be addressed to Elena A. Plis; elena.plis@gmail.com

Received 5 January 2014; Accepted 19 March 2014; Published 10 April 2014

Academic Editor: Meiyong Liao

InAs/(In,Ga)Sb type-II strained layer superlattices (T2SLs) have made significant progress since they were first proposed as an infrared (IR) sensing material more than three decades ago. Numerous theoretically predicted advantages that T2SL offers over present-day detection technologies, heterojunction engineering capabilities, and technological preferences make T2SL technology promising candidate for the realization of high performance IR imagers. Despite concentrated efforts of many research groups, the T2SLs have not revealed full potential yet. This paper attempts to provide a comprehensive review of the current status of T2SL detectors and discusses origins of T2SL device performance degradation, in particular, surface and bulk dark-current components. Various approaches of dark current reduction with their pros and cons are presented.

1. Introduction

Since proposed in 1980s [1–3], the InAs/(In,Ga)Sb T2SL has gained a lot of interest for the infrared (IR) detection applications. Focal plane arrays (FPAs) based on T2SL and operating in mid-wave IR (MWIR, 3–5 μm) and long-wave IR (LWIR, 8–12 μm) are of great importance for a variety of civil and military applications. Currently market dominating technologies are based on bulk mercury cadmium telluride (MCT) and InSb [4–6], and GaAs/AlGaAs quantum well IR photodetectors (QWIPs).

While MCT detectors have very large quantum efficiency (>90%) and detectivity, they are still plagued by nonuniform growth defects and a very expensive CdZnTe substrate that is only available in limited quantities by a foreign manufacturer. There has been significant progress on development of MCT on silicon substrates, but good performance has been limited to the MWIR band only. Moreover, MCT is characterized by low electron effective mass resulting in excessive leakage current [7]. The InSb detectors do not cover the LWIR spectral range. QWIPs are based on III-V semiconductors and their mature manufacturing process enables them to be scaled to large format FPAs with a high degree of spatial uniformity [8–10]. However, due to polarization selection rules for electron-photon interactions in GaAs/AlGaAs QW, this material system is insensitive to surface-normal incident IR radiation resulting in poor conversion quantum efficiency, In addition, their large dark currents lower the operating temperature and increase the operating cost of the imager. The development of FPAs based on mature III-V growth and fabrication technology and operating at higher temperatures will result in highly sensitive, more reliable, lighter, and less costly IR sensors than currently available ones.

The InAs/(In,Ga)Sb T2SL material system is characterized by a broken-gap type-II alignment schematically illustrated in Figure 1 with electron and hole wavefunctions having maxima in InAs and GaSb layers, respectively. The overlap of electron (hole) wave functions between adjacent InAs (GaSb) layers result in the formation of an electron (hole) minibands in the conduction (valence) band. Optical transition between the highest hole (heavy-hole) and the lowest conduction minibands is employed for the detection of incoming IR radiation. The operating wavelength of the T2SLs can be tailored from 3 μm to 32 μm by varying thickness of one or two T2SL constituent layers [11–13]. Some parameters of T2SL constituent materials, InAs and GaSb, are shown in Table 1.

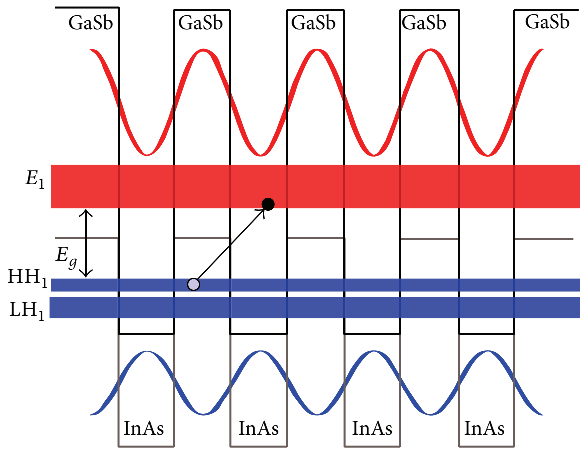

FIGURE 1: Type-II band alignment of InAs/GaSb T2SL system.

TABLE 1: Some band structure parameters for InAs and GaSb (0 K).

Parameter	InAs	Reference	GaSb	Reference
E_g^{Γ} (eV)	0.417	[14]	0.812	[15]
E_g^{X} (eV)	1.433	[16]	1.141	[17]
E_g^{L} (eV)	1.133	[18]	0.875	[19]
m_e^* (Γ)	0.026	[20]	0.039	[16]
m_l^* (L)	0.640	[21, 22]	1.30	[23, 24]
m_t^* (L)	0.050	[21, 22]	0.100	[23, 24]
m_l^* (X)	1.130	[21, 22]	1.510	[23, 24]
m_t^* (X)	0.160	[21, 22]	0.220	[23, 24]

InGaSb layers of InAs/InGaSb T2SL are subjected to biaxial compression strain causing splitting of light hole and heavy-hole minibands in the T2SL band structure and, therefore, suppression of Auger recombination rates relative to bulk MCT detectors [25, 26]. However, the majority of the research in the past ten years has focused on the binary InAs/GaSb system. This is attributed to the critical thickness limitations imposed on strained material grown with the large mole fraction of In. The scope of this paper is also limited to the InAs/GaSb T2SL devices.

1.1. Characterization of T2SL Material System. The physics behind the T2SL material system is not yet very well understood. Different theoretical methods have been applied to understand the band structure, electronic, and optical properties of superlattices. For example, Flatté et al. have undertaken extensive theoretical modeling of the band structure of superlattices [27–29], including investigation of electronic structure of dopants [30]. Features of T2SL photoabsorption spectra and optical properties of T2SL detectors were studied by Livneh et al. [31] and Qiao et al. [32], respectively, using k · p tight-binding model [33]. Empirical pseudopotential method, in its canonical shape [34–36] and four-component variation that includes interface layers [37], was successfully utilized for the heterojunction design of T2SL devices. Bandara et al. [38] have modeled the effect of doping on the Shockley-Read-Hall (SRH) lifetime and the dark current; Pellegrino and DeWames [39] have performed extensive modeling to extract the SRH lifetime from dark-current measurements.

Background carrier concentration is one of the fundamental properties of the absorber layer of T2SL detector since it determines the minority carrier lifetime and diffusion lengths. Transport measurements in T2SL are difficult because of the lack of semi-insulating GaSb substrates. Several techniques have been reported to measure and analyze the electrical properties of T2SL by different groups. Magneto-transport analysis [40] was performed on T2SL structures grown on top of electrically insulating AlGaAsSb buffer in order to suppress parasitic conduction. Hall [41], capacitance-voltage, and current-voltage measurements [42] of T2SL structures grown on semi-insulating GaAs substrate directly or with the interfacial misfit (IMF) dislocation arrays technique [43] were also reported. Variable magnetic field geometric magnetoresistance measurements and a mobility spectrum analysis, (MSA) technique for data analysis, have been employed by Umana-Membreno et al. [44] to study vertical minority carrier electron transport parameters in T2SL structures. Works of Christol et al. [45, 46], Haugan et al. [47], and Szmulowicz et al. [48, 49]are concerned with the influence of T2SL composition and growth conditions on background carrier concentration and mobility.

Since performance of T2SL device is strongly dependent on T2SL structural perfection, the information on interfacial roughness, compositional profile (i.e., interfacial intermixing), and interfacial bonding across the noncommon anion layers of InAs/GaSb T2SL is very important. Growth conditions of T2SLs have been optimized by various research groups to improve the interface quality [50–54]. Steinshnider and colleagues [55–58] utilized the cross-sectional scanning tunneling microscopy (XSTM) to identify the interfacial bonding and to facilitate direct measurements of the compositional grading at the GaSb/InAs heterojunction. *In situ* study of origins of interfacial disorder and cross-contamination in T2SL structures [59, 60] revealed importance of Arsenic (As) background pressure control during the GaSb layers growth. Luna et al. [61] proposed the method of systematic characterization of InAs-on-GaSb and GaSb-on-InAs interfaces in T2SL with resolution less than 0.5 nm.

1.2. InAs/GaSb T2SL Detectors. T2SL diodes are predicted to have a number of advantages over bulk MCTs, including lower tunneling current, since the band edge effective masses in T2SL are not directly dependent on the band gap energy and are larger than HgCdTe at the same band gap [3]. The band-engineered suppression of Auger recombination rates [25, 26] leads to improved temperature limits of spectral detectivities. In contrast with QWIPs, normal incidence absorption is permitted in T2SLs, contributing to high conversion quantum efficiencies. Moreover, the commercial availability of substrates with good electrooptical homogeneity, and without large cluster defects, also offers advantages for T2SL technology. Thorough comparisons between MCT, InSb, QWIP, and T2SL technologies can be found in the literature [62–65].

Table 2: Properties of MWIR and LWIR T2SL detectors at 77 K [88, 89].

Parameter	MWIR T2SL $\lambda_{\text{Cut-off}} = 5\,\mu$m	LWIR T2SL $\lambda_{\text{Cut-off}} = 10\,\mu$m
Quantum efficiency (%)	~70	~70
R_0A ($\Omega\cdot$cm^2)	10^6	10^3
Detectivity (Jones) FOV = 0	1×10^{14}	6×10^{11}

Table 3: Properties of MWIR and LWIR T2SL FPAs at 77 K [90–92].

Parameter	MWIR T2SL $\lambda_{\text{Cut-off}} = 5\,\mu$m	LWIR T2SL $\lambda_{\text{Cut-off}} = 10\,\mu$m
Format	320 × 256	1024 × 1024
Quantum efficiency (%)	~50	~50
NEDT (mK)	>15	~30

High performance InAs/GaSb T2SL detectors have been reported for MWIR [66–68], LWIR [12, 69–72], and very-long wave IR (VLWIR) [73, 74] spectral regions. Moreover, mega-pixel FPAs, that is, FPAs of sizes up to 1024 × 1024, have been demonstrated [75, 76]. Multiband T2SL structures were realized, including short-wave IR (SW)/MWIR [77], MW/MWIR [78], MW/LWIR [79, 80], LW/LWIR [81], and SW/MW/LWIR [82] devices. Low-dark-current architectures with unipolar barriers such as M-structure [83], complementary-barrier infrared detector (CBIRD) [70], W-structure [69, 84], N-structure [85], nBn [86, 87], and pBiBn [12] have been designed and fabricated into single-pixel detectors and FPAs at university laboratories (Northwestern University, Arizona State University, University of Oklahoma, University of Illinois, Georgia Tech University, Bilkent University (Turkey), University of New Mexico), federal laboratories (JPL, NRL, ARL, NVESD, and SNL), and industrial laboratories (Raytheon, Teledyne Imaging Systems, Hughes Research Laboratories, QmagiQ LLC, etc.). Tables 2 and 3 summarize properties of MWIR and LWIR T2SL detectors and FPAs at 77 K.

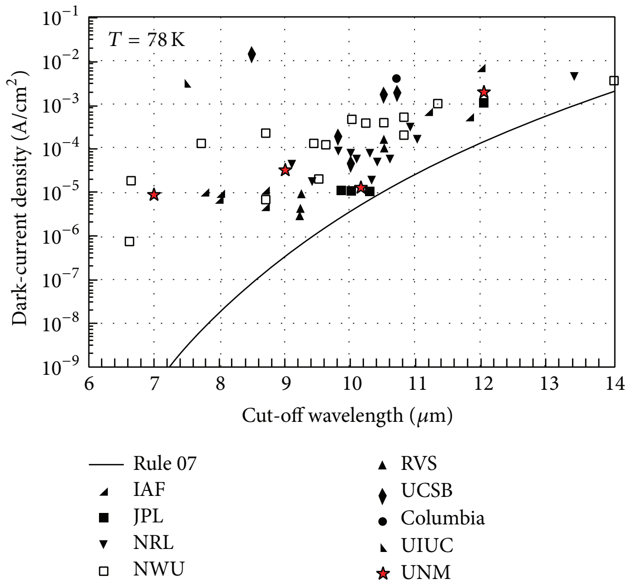

Figure 2: Dark-current density of T2SL detectors compared with Rule 07 [93]. Abbreviations for the different institution working on T2SL detectors: Fraunhofer-Institut (IAF), Jet Propulsion Laboratory (JPL), Naval Research Laboratory (NRL), Northwestern University (NWU), Raytheon Vision Systems (RVS), University of California, Santa Barbara (UCSB), Columbia University (Columbia), University of Illinois, Urbana-Champaign (UIUC), and University of New Mexico (UNM).

2. Limitations of T2SL Technology

Despite the numerous technological and theoretically predicted advantages T2SLs offer over present-day detection technologies, the promise of superior performance of T2SL detectors has not been yet realized. The T2SL detectors are approaching the empirical benchmark of MCT's performance level, Rule 07 [93]; however, the dark-current density demonstrated by the T2SL detectors is still significantly higher than that of bulk MCT detectors, especially in the MWIR range, as illustrated in Figure 2.

To understand the reasons of high dark-current levels demonstrated by the T2SL detectors the origins of dark current have to be analyzed. Generally, dark current in detectors based on narrow band gap semiconductors may be differentiated into "bulk" and "surface" currents. The most important "bulk" dark currents are (i) generation-recombination (G-R) current associated with the SRH process in the depletion region of the detector and (ii) thermally generated diffusion current associated with Rogalski [94] or radiative process in both the n- and p-extrinsic regions of the detector [95].

The SRH G-R process occurs through the trap levels within the energy gap thus limiting lifetime of the minority carriers. The origins of SRH centers are not well understood. According to the statistical theory of the SRH process, the SRH rate approaches a maximum as the energy level of the trap center approaches midgap. Thus, the most effective SRH centers are those located near the middle of the band gap [96]. Analysis of the defect formation energy of native defects dependent on the location of the Fermi level stabilization energy has been performed by Walukiewicz [97], who reported that, in bulk GaAs and GaSb, the stabilized Fermi level is located near either the valence band or the midgap, whereas in bulk InAs the stabilized Fermi level is located above the conduction band edge. From this observation, the midgap trap levels in GaAs and GaSb are available for SRH recombination, whereas in InAs they are inactive for the SRH process, suggesting a longer carrier lifetime in bulk InAs than in bulk GaSb and GaAs materials. Experimentally measured values of carrier lifetimes yielded ~325 ns for bulk InAs and ~100 ns for bulk GaSb, thereby confirming the initial observation [98]. It may then be hypothesized that native defects associated with GaSb are responsible for the SRH-limited minority-carrier lifetimes observed in InAs/GaSb T2SL.

Several methods have been employed to measure lifetime of photogenerated carriers of T2SL, including optical modulation response [38, 47], time-resolved PL [99–102], and photoconductive response variation measurements [103], to name just a few. Some of them provide more direct measures of lifetime, while others rely on assumptions or further measurements to perform extraction of lifetime [39, 104, 105]. Overall, the lifetimes reported for MWIR and LWIR InAs/GaSb T2SL range from 0.13 ns [106] to about 100 ns [107]. These values are significantly lower compared to the MCT devices operating in the same wavelength range [107].

A "surface" dark current component is associated with the surface states in the junction. During the individual pixel isolation process, the periodic crystal structure terminates abruptly resulting in formation of unsatisfied (dangling) chemical bonds at the semiconductor-air interface responsible for generation of surface states within the band gap and pinning of the Fermi level. Moreover, etch by-products, surface contaminant associated with the fabrication procedure, and differential etching also create additional interfacial states contributing to the dark current. Scaling of the lateral dimensions of a T2SL detector (e.g., typical mesa dimensions of individual FPA pixels are 20 μm × 20 μm) makes FPA performance strongly dependent on surface effects due to a large pixel surface/volume ratio.

This paper aims to review various ways of improving performance of T2SL detectors in order for T2SLs to be the technology of choice for high-performance IR imaging systems. Proposed solutions for the reduction of "bulk" and "surface" dark-current components as well as improvement of detector signal-to-noise ratio and operating temperature limits will be discussed in detail.

3. Proposed Solutions for the Improvement of T2SL Detector Performance

3.1. Reduction of "Bulk" Dark Currents. To overcome the carrier lifetime limitations imposed by the GaSb layer in an InAs/GaSb T2SL, the type-II Ga-free SL, that is, InAs/InAsSb SL, may be utilized for IR detection. A significantly longer minority carrier lifetime has been obtained in an InAs/InAsSb SL system as compared to an InAs/GaSb T2SL operating in the same wavelength range (at 77 K, ~412 ns, and ~100 ns, resp.) [100, 108]. Such increases in minority carrier lifetimes, along with demonstrated band gap adjustability [109] and suppressed Auger recombination rates [110], suggest lower dark currents for InAs/InAsSb SL detectors in comparison with their InAs/GaSb T2SL counterparts. However, performance, in particular, signal-to-noise ratio, of InAs/InAsSb SL-based detectors with pin [111] and nBn [112] architectures was not superior to T2SL-based devices operating in the same wavelength range. This may be attributed to the increased tunneling probability in InAs/InAsSb SL system due to the smaller band offsets [111] and significant concentration of SRH centers in this material [113].

Thermally generated diffusion currents may be significantly suppressed by the incorporation of barriers into conduction and valence bands to impede the flow of carriers associated with dark current (noise) without blocking photocurrent (signal). The improved performance of these T2SL devices is credited to better confinement of the electron wavefunctions, reduced tunneling probability, increased electron effective mass in modified T2SL structures, and reduction in dark-current through the use of current blocking layers that reduce one or more dark-current component. nBn [86, 87], pBiBn [12], M-structure [83], W-structure [84], CBIRD [70], and N-structure [85] are examples of T2SL detectors with barrier architecture.

The band-offset tunability is critical parameter for the realization of barrier devices. Barrier layers are selected such that the hole-blocking layer offers an unimpeded electrons flow while blocking holes and electron-blocking layer fulfill the opposite function. Hence, one requires hole- (electron) blocking layers to have zero valence (conduction) band offsets with the absorber layer. Moreover, for the efficient barrier structure design, complete macroscopic simulations are required to get a good assessment of actual dark current and photocurrent. This simulation may as well help with design optimization of barrier structures, in particular, selecting an optimal barriers thickness, composition, and doping concentration.

The extension of concept of heterostructure barrier engineering in T2SL resulted in realization of interband cascade infrared photodetectors (ICIPs) [114–118]. In ICIP detectors each cascade stage is comprised of an absorber region, relaxation region, and interband tunneling region. While photocurrent is limited to the value produced in an individual absorber, adding of extra- stages benefits the signal-to-noise ratio, since the noise current in such devices scales inversely with the total number of stages. Ability to change number of stages with different absorber thicknesses is important for the design of T2SL detectors with maximized signal-to-noise ratio. The drawbacks of ICIPs are associated with the complicated structure of these devices. In particular, due to the number of layers and interfaces in the structure, some of the fundamental device physics is still unclear and MBE growth procedure is challenging.

Ability to heteroengineer the band structure of the T2SL devices stipulates realization of one more type of low-noise T2SL detectors, avalanche photodiodes (APDs) [119–121]. Control of individual layer thickness and composition offers great flexibility in engineering of the electron band structure to initiate single-carrier ionization. Moreover, APDs with either electron or hole dominated avalanching may be fabricated by engineering the higher lying T2SL energy levels. It should be noted that an APD device with hole dominating avalanching is expected to have lower noise due to reduced tunneling of heavier holes. Existence of hole dominated avalanching structure also opens up possibility of combining separate electron and hole multiplication regions in a single device achieving very high gain with low excess noise factor.

3.2. Reduction of "Surface" Dark Currents. Despite numerous efforts of various research groups devoted to the development of effective passivation schemes for T2SL detectors, there is still no well-established and generally acknowledged procedure for passivation of such devices. Part of the problem is the complexity of T2SL system, composed by the hundreds of relatively thick (several monolayers, MLs) InAs, GaSb, and, sometimes, AlSb layers, and thin (typically, less than 1 ML) interfacial GaAs and InSb layers [55, 57, 58, 122]. Passivation should satisfy dangling bonds of all these T2SL constituent materials, originated at exposed device sidewalls after mesa definition process, and prevent formation of interface states in the T2SL band gap.

The great advantage of T2SL system, band gap tunability, allowing realization of detectors spanning wide IR range, serves as a disservice for the passivation development. Interface states cause the pinning of Fermi level with the bands bend towards lower energy near the surface. This band bending induces accumulation or type inversion of charge resulting in surface tunneling currents along sidewalls. As was shown by Delaunay et al. [123], the narrow band gap devices (LWIR and VLWIR, with band gap of 120 meV or lower) are more susceptible to the formation of charge conduction channels along the sidewalls. Consequently, the same passivation may be suitable for the T2SL MWIR and inefficient for the T2SL detectors with longer operating wavelength.

Moreover, passivation should exhibit thermal and long term stability. In other words, passivation layer must not undergo any change in its constitutional, physical, and interfacial properties at variable temperatures (30–300 K) during the lifetime of the T2SL detector (typically, 10,000 hrs). Finally, passivation has to be easily integrated into the FPA fabrication process.

In addition, since passivation applied on rough surfaces, or surfaces contaminated by native oxides, and foreign particles will result in little or no improvement of device performance, we spent some time discussing the surface preparation issues. To achieve minimal surface leakage, the device sidewalls must be smooth, with no patterns of preferential etch presented, and clean, with removed native oxides and etch by-products. Moreover, vertical etch profile is essential for the realization of high-fill factor, small pixel pitch, and large format T2SL FPAs. The thorough comparisons of various surface preparation and passivation techniques of T2SL detectors are out of the scope of this review article and can be found in literature [124, 125]. Next two sections aim to familiarize the reader with various mesa definition and passivation methods developed for T2SL devices.

3.2.1. Surface Preparation. Definition of nearly vertical mesa sidewalls that are free of native oxide and defects is the crucial step in InAs/GaSb T2SL detector fabrication process [126, 127]. Presence of elemental antimony on the etched T2SL device sidewalls [128] may result in the conduction channel parallel to the interface, which leads to increasing of surface component of dark current. Unwanted native oxides are usually removed prior to or during the pixel isolation process with immersion in ammonium sulfide [127], phosphoric or hydrochloric acid based solutions [129]. Introduction of BCl_3 gas into the plasma chemistry is also effective in removal of native oxides and redeposited by-products [130].

Nowadays, high-density plasma etch processes are commonly utilized for InAs/GaSb T2SL material in spite of inevitable degradation of sidewall surface electronic properties due to ion bombardment or unwanted deposition of etch by-products [131, 132]. Plasma chemistry usually consists of chlorine-based precursors (BCl_3, Cl_2, or $SiCl_2$) due to high volatilities of gallium, indium, antimony, and arsenide chlorides providing fast etch rates and smooth morphologies [133]. The resulting etch profiles are vertical due to the plasma sheath and the ionized gas directionality. Damage produced during the dry etch may be partially restored by subsequent chemical treatment [134]. Due to the ability of wet etches to cause virtually no surface electronic damage, a chemical etch attracts attention of researchers for single-pixel T2SL device fabrication [135–140]. However, the isotropic nature of wet etch process resulting in concave sidewall profile and an unavoidable tendency to undercut etch masks making precise dimensional control more difficult stipulates limited application of wet etches for T2SL FPA fabrication.

3.2.2. Passivation. Conventional passivation methods of T2SL devices include encapsulation of device sidewalls, by thick layer of dielectric or organic material, and sulfidization. Dielectric passivation of T2SL detectors is compatible with current T2SL FPA fabrication procedures and, consequently, very appealing to the T2SL scientists and engineers. Numerous reports on passivation of MWIR and LWIR T2SL detectors by silicon oxide or silicon nitride have been published over the last fifteen years [74, 81, 130, 141–144]. Dielectric passivation, though shown to be effective, presents the challenges of developing high-quality, low fixed, and interfacial charges density dielectrics at process temperatures substantially lower that the InAs/GaSb T2SL growth temperature to prevent the T2SL period intermixing. Moreover, native fixed charges presented in dielectric passivation layer can either improve or deteriorate the device performance [143]; consequently, the dielectric passivation may not passivate the low band gap materials as effectively as high band gap materials.

T2SL passivation with organic materials, which are polyimide or various photoresists (PRs), is emerging alternative to the dielectric passivation approach [134, 135, 145–150]. PRs are commonly deposited at room temperature and thus the T2SL thermal budget is not exerted. Moreover, PRs equally effectively passivate T2SL detectors with different operating wavelengths.

Chalcogenide passivation, or saturation of unsatisfied bonds on semiconductor surface by sulfur atoms, has been employed from early 1990s for the passivation of bulk III-V materials [151–162]. The enhanced photoluminescence (PL) and reduced diode leakage current were credited to the formation of III-S bond responsible for the reduction of surface states within band gap.

The simplest sulfidization scheme of T2SL detectors is device immersion in aqueous solution of ammonium sulfide. No native oxide removal step is required prior to passivation because the native oxides are etched by $(NH_4)OH$ formed in water solution of ammonium sulfide. Short-term benefits for the MWIR and LWIR T2SL device performance have been reported [127, 129, 163] and the necessity for a suitable capping layer to preserve good passivation quality in the long term was reaffirmed. Thioacetamide (TAM, C_2H_5NS) [124, 164] and octadecanethiol (ODT, $CH_3[CH_2]_{17}SH$) [85] treatments offer formation of more stable bonds between sulfur and T2SL constituent elements (Ga, In, As, and Sb) compared to weaker III (V)-oxygen-S bonds formed after ammonium sulfide treatment.

One of relatively new sulfidization methods is electrochemical passivation (ECP) [129, 165] that is saturation of dangling bonds with sulfur through electrolysis in S-containing solution. Though effective, sulfur layer deposited through ECP may oxidize easily and additional encapsulation is required. Electron-beam evaporated ZnS satisfies the dangling bonds with S-atoms simultaneously acting as an encapsulant [119–121, 166].

Recently, several research groups reported the "combined" approach for the passivation of T2SL detectors. For example, Zhang et al. [167] noticed that the anodic sulfide passivation combined with the SiO_2 significantly improved the performance of MWIR T2SL detectors. DeCuir Jr. et al. [147] found that the sulfide chemical treatment followed by the SU-8 treatment inhibits the formation of native surface oxides, satisfies dangling bonds, and prevents the sulfide layer degradation over time.

4. Other Methods of T2SL Detector Performance Improvement

The bulk components of the dark current (SRH and thermally generated diffusion current) in T2SL detector may be significantly diminished by scaling thickness of the device. The abridged quantum efficiency (QE) of such device may be restored through plasmon assisted coupling of incident electromagnetic radiation while maintaining low dark-current level. Transmission enhancement and QE increase through subwavelength metal hole array [168] and corrugated metal surface structure [169], respectively, have been reported for MWIR T2SL detectors.

Surface currents may be suppressed by reduced exposure of narrow gap materials to the environment, for example, as a result of encapsulation of etched sidewalls with wide band gap material [133, 170] or buried architecture [84] that isolates the neighboring devices but terminates within a wider band gap layer. The former passivation approach requires very careful surface cleaning prior the overgrowth procedure, whereas latter is subjected to the possible crosstalk issues in FPAs due to the uncertainty of the lateral diffusion length of minority carriers. If the values of lateral diffusion length are larger than the distance between neighboring pixels in the FPA, crosstalk between the FPA elements can be encountered that leads to the degradation of image resolution.

Another approach for the realization of high performance T2SL sensors is growth of T2SL structures on high-index plane GaSb [171]. The thickness of the T2SL detector grown on the GaSb (111) substrate is reduced due to the natural difference of lattice parameters in the (111) and (100) directions, whereas heavy hole confinement is increased by a factor of three [172]. This translates into thinner detector structures for a given detection wavelength and absorption coefficient realized on (111) GaSb substrate, resulting in shorter growth times. This also means decreased costs and material usage, both of which are highly desirable. Moreover, the decreased detector volume results in an improved signal-to-noise ratio, since the number of thermally generated carriers is correspondingly reduced.

5. Summary

This work provides a review of the current status and limitations of IR detectors based on an InAs/GaSb T2SLs. It should be noted that applications of T2SL system are not limited to the IR detection only. Low thermal conductivity of T2SL identifies it as a prospective material for low-temperature Peltier coolers [173]. Spatially separated confinement of electrons and holes, signature of type-II band alignment, initiated InAs/GaSb core-shell nanowires realization [174, 175]. Field-effect transistors (FETs) [176, 177] and thermo photovoltaic (TPV) [178] T2SL devices are another examples of unconventional applications of T2SL material system.

Despite the numerous theoretically predicted advantages that T2SLs offer over MCT, InSb, and QWIP-based detectors, intensive heterostructure engineering efforts and development of epitaxial growth and fabrication techniques, the promise of superior performance of T2SL detectors has not been yet realized. The dark-current density demonstrated by the T2SL detectors is still significantly higher than that of bulk MCT detectors, especially in the MWIR range.

The complexity of T2SL system, along with the intricate detector architectures, results in no universal solution for the suppression of dark currents. Different approaches that address suppression of either bulk or surface dark current components in order for T2SL to be the technology of choice for high-performance imaging systems have been presented.

The SRH and thermally generated diffusion currents may be significantly reduced by exclusion of GaSb layer from InAs/GaSb T2SL stack, that is, Ga-free T2SL, and by the incorporation of barriers device structure to impede the flow of carriers associated with dark current (noise) without blocking photocurrent (signal), respectively. Passivation treatment of the exposed device sidewalls decreases the surface currents. However, development of effective passivation technique is hindered by the ease of native oxide formation and requirements to the etched surface. In addition, the same passivation may be suitable for the T2SL MWIR and inefficient for the T2SL detectors with longer operating wavelength. Finally, one of the most effective passivation approaches, saturation of unsatisfied chemical bonds with sulfur atoms, results in formation of passivation layer with poor long-term stability, and additional encapsulation is required.

Integration of T2SL detectors with surface plasmon couplers and utilization of high-index plane GaSb substrates are recent alternatives for the improvement of T2SL detector performance. Despite the promising preliminary results, both of these directions require additional investigation.

In conclusion, unique combination of band structure engineering flexibility and material properties of InAs/GaSb T2SL provide a prospective benefit in the realization of next generation IR imagers. Performance of MWIR and LWIR T2SL detectors has not achieved its theoretically predicted limit. To fully realize the T2SL potential methods of suppression of various dark current components have to be developed. Up-to-date techniques of dark current reduction include not only traditional passivation, but advanced heterostructure engineering and integration of T2SL with nanostructures as well.

Conflict of Interests

The author declares that there is no conflict of interests regarding the publication of this paper.

Acknowledgments

This work was supported by the AFOSR FA9550-10-1-0113 and AFRL FA9453-12-1-0336 Grants.

References

[1] G. A. Sai-Halasz, R. Tsu, and L. Esaki, "A new semiconductor superlattice," *Applied Physics Letters*, vol. 30, no. 12, pp. 651–653, 1977.

[2] L. Esaki, "InAs-GaSb superlattices-synthesized semiconductors and semimetals," *Journal of Crystal Growth*, vol. 52, no. 1, pp. 227–240, 1981.

[3] D. L. Smith and C. Mailhiot, "Proposal for strained type II superlattice infrared detectors," *Journal of Applied Physics*, vol. 62, no. 6, pp. 2545–2548, 1987.

[4] J. Rothman, E. D. Borniol, P. Ballet et al., "HgCdTe APD-Focal plane array performance at DEFIR," in *Infrared Technology and Applications XXXV*, vol. 7298 of *Proceedings of SPIE*, pp. 729835–729845, April 2009.

[5] J. M. Peterson, D. D. Lofgreen, J. A. Franklin et al., "MBE growth of HgCdTe on large-area Si and CdZnTe wafers for SWIR, MWIR and LWIR detection," *Journal of Electronic Materials*, vol. 37, no. 9, pp. 1274–1282, 2008.

[6] O. Nesher, I. Pivnik, E. Ilan et al., "High resolution 1280×1024, 15 μm pitch compact InSb IR detector with on-chip ADC," in *Infrared Technology and Applications XXXV*, vol. 7298 of *Proceedings of SPIE*, April 2009.

[7] A. Rogalski, "HgCdTe infrared detector material: history, status and outlook," *Reports on Progress in Physics*, vol. 68, no. 10, pp. 2267–2336, 2005.

[8] H. Schneider and H. C. Liu, *Quantum Well Infrared Photodetectors*, Springer Series in Optical Sciences, Springer, 2007.

[9] A. Soibel, S. V. Bandara, D. Z. Ting et al., "A super-pixel QWIP focal plane array for imaging multiple waveband temperature sensor," *Infrared Physics and Technology*, vol. 52, no. 6, pp. 403–407, 2009.

[10] A. Nedelcu, V. Guériaux, A. Bazin et al., "Enhanced quantum well infrared photodetector focal plane arrays for space applications," *Infrared Physics and Technology*, vol. 52, no. 6, pp. 412–418, 2009.

[11] C. Cervera, I. Ribet-Mohamed, R. Taalat, J. P. Perez, P. Christol, and J. B. Rodriguez, "Dark current and noise measurements of an InAs/GaSb superlattice photodiode operating in the midwave infrared domain," *Journal of Electronic Materials*, vol. 41, pp. 2714–2718, 2012.

[12] N. Gautam, H. S. Kim, M. N. Kutty, E. Plis, L. R. Dawson, and S. Krishna, "Performance improvement of longwave infrared photodetector based on type-II InAs/GaSb superlattices using unipolar current blocking layers," *Applied Physics Letters*, vol. 96, no. 23, Article ID 231107, 2010.

[13] Y. Wei, A. Gin, M. Razeghi, and G. J. Brown, "Advanced InAs/GaSb superlattice photovoltaic detectors for very long wavelength infrared applications," *Applied Physics Letters*, vol. 80, no. 18, pp. 3262–3264, 2002.

[14] Y. Lacroix, C. A. Tran, S. P. Watkins, and M. L. W. Thewalt, "Low-temperature photoluminescence of epitaxial InAs," *Journal of Applied Physics*, vol. 80, no. 11, pp. 6416–6424, 1996.

[15] P. S. Dutta, H. L. Bhat, and V. Kumar, "The physics and technology of gallium antimonide: an emerging optoelectronic material," *Journal of Applied Physics*, vol. 81, no. 9, pp. 5821–5870, 1997.

[16] M. Levinshtein, S. Rumyantsev, and M. Shur, Eds., *Handbook Series on Semiconductor Parameters*, vol. 1 and 2, World Scientific, 1996.

[17] A. Joullié, A. Z. Eddin, and B. Girault, "Temperature dependence of the $L_6^c - \Gamma_6^c$ energy gap in gallium antimonide," *Physical Review B*, vol. 23, no. 2, pp. 928–930, 1981.

[18] E. Adachi, "Energy band parameters of InAs at various temperatures," *Journal of the Physical Society of Japan*, vol. 24, no. 5, p. 1178, 1968.

[19] C. Alibert, A. Joullie, and A. M. Joullie, "Modulation-spectroscopy study of the GaAlSb band structure," *Physical Review B*, vol. 27, p. 4946, 1983.

[20] M. B. Thomas and J. C. Woolley, "Plasma edge reflectance measurements in GaInAs and InAsSb alloys," *Canadian Journal of Physics*, vol. 49, p. 2052, 1971.

[21] D. C. Tsui, "Landau-level spectra of conduction electrons at an InAs surface," *Physical Review B*, vol. 12, no. 12, pp. 5739–5748, 1975.

[22] R. A. Stradling and R. A. Wood, "The temperature dependence of the band-edge effective masses of InSb, InAs and GaAs as deduced from magnetophonon magnetoresistance measurements," *Journal of Physics C: Solid State Physics*, vol. 3, no. 5, article 005, pp. L94–L99, 1970.

[23] C. Ghezzi, R. Magnanini, A. Parisini et al., "Optical absorption near the fundamental absorption edge in GaSb," *Physical Review B*, vol. 52, no. 3, pp. 1463–1466, 1995.

[24] H. Arimoto, N. Miura, R. J. Nicholas, N. J. Mason, and P. J. Walker, "High-field cyclotron resonance in the conduction bands of GaSb and effective-mass parameters at the L points," *Physical Review B*, vol. 58, no. 8, pp. 4560–4565, 1998.

[25] E. R. Youngdale, J. R. Meyer, C. A. Hoffman et al., "Auger lifetime enhancement in InAs-$Ga_{1-x}In_xSb$ superlattices," *Applied Physics Letters*, vol. 64, no. 23, pp. 3160–3162, 1994.

[26] G. M. Williams, "Comment on "Temperature limits on infrared detectivities of $InAs/In_xGa_{1-x}Sb$ superlattices and bulk Hg_xCd_{1-x} Te" [J. Appl. Phys. 74, 4774 (1993)]," *Journal of Applied Physics*, vol. 77, no. 8, pp. 4153–4155, 1995.

[27] M. E. Flatté, C. H. Grein, H. Ehrenreich, R. H. Miles, and H. Cruz, "Theoretical performance limits of 2.1-4.1 μm InAs/InGaSb, HgCdTe, and InGaAsSb lasers," *Journal of Applied Physics*, vol. 78, no. 7, pp. 4552–4561, 1995.

[28] K. Abu El-Rub, C. H. Grein, M. E. Flatte, and H. Ehrenreich, "Band structure engineering of superlattice-based short-, mid-, and long-wavelength infrared avalanche photodiodes for improved impact ionization rates," *Journal of Applied Physics*, vol. 92, no. 7, pp. 3771–3778, 2002.

[29] M. E. Flatté and C. H. Grein, "Theory and modeling of type-II strained-layer superlattice detectors," in *Quantum Sensing and Nanophotonic Devices VI*, vol. 7222 of *Proceedings of SPIE*, January 2009.

[30] M. E. Flatté and C. E. Pryor, "Defect states in type-II strained-layer superlattices," in *Quantum Sensing and Nanophotonic Devices VII*, vol. 7608 of *Proceedings of SPIE*, January 2010.

[31] Y. Livneh, P. Klipstein, O. Klin et al., "kp model for the energy dispersions and absorption spectra of InAs/GaSb type-II superlattices," *Physical Review B*, vol. 86, Article ID 235311, 2012.

[32] P.-F. Qiao, S. Mou, and S. L. Chuang, "Electronic band structures and optical properties of type-II superlattice photodetectors with interfacial effect," *Optics Express*, vol. 20, no. 3, pp. 2319–2334, 2013.

[33] P. C. Klipstein, "Operator ordering and interface-band mixing in the Kane-like Hamiltonian of lattice-matched semiconductor superlattices with abrupt interfaces," *Physical Review B*, vol. 81, no. 23, Article ID 235314, 2010.

[34] G. C. Dente and M. L. Tilton, "Pseudopotential methods for superlattices: applications to mid-infrared semiconductor lasers," *Journal of Applied Physics*, vol. 86, no. 3, pp. 1420–1429, 1999.

[35] R. Kaspi, C. Moeller, A. Ongstad et al., "Absorbance spectroscopy and identification of valence subband transitions in type-II InAs/GaSb superlattices," *Applied Physics Letters*, vol. 76, no. 4, pp. 409–411, 2000.

[36] G. C. Dente and M. L. Tilton, "Comparing pseudopotential predictions for InAs/GaSb superlattices," *Physical Review B*, vol. 66, no. 16, Article ID 165307, 2002.

[37] J. M. Masur, R. Rehm, J. Schmitz, L. Kirste, and M. Walther, "Four-component superlattice empirical pseudopotential method for InAs/GaSb superlattices," *Infrared Physics & Technology*, vol. 61, pp. 129–133, 2013.

[38] S. Bandara, P. G. Maloney, N. Baril, J. G. Pellegrino, and M. Z. Tidrow, "Doping dependence of minority carrier lifetime in long-wave Sb-based type II superlattice infrared detector materials," *Optical Engineering*, vol. 50, no. 6, Article ID 061015, 2011.

[39] J. Pellegrino and R. DeWames, "Minority carrier lifetime characteristics in type II InAs/GaSb LWIR superlattice n+πp+ photodiodes," in *Infrared Technology and Applications XXXV*, vol. 7298 of *Proceedings of SPIE*, April 2009.

[40] L. Bürkle, F. Fuchs, J. Schmitz, and W. Pletschen, "Control of the residual doping of InAs/(GaIn)Sb infrared superlattices," *Applied Physics Letters*, vol. 77, no. 11, pp. 1659–1661, 2000.

[41] X. B. Zhang, J. H. Ryou, R. D. Dupuis et al., "Improved surface and structural properties of InAs/GaSb superlattices on (001) GaSb substrate by introducing an InAsSb layer at interfaces," *Applied Physics Letters*, vol. 90, no. 13, Article ID 131110, 2007.

[42] X. B. Zhang, J. H. Ryou, R. D. Dupuis et al., "Metalorganic chemical vapor deposition growth of high-quality InAsGaSb type II superlattices on (001) GaAs substrates," *Applied Physics Letters*, vol. 88, no. 7, Article ID 072104, 2006.

[43] A. Jallipalli, G. Balakrishnan, S. H. Huang et al., "Structural analysis of highly relaxed GaSb grown on GaAs substrates with periodic interfacial array of 90° misfit dislocations," *Nanoscale Research Letters*, vol. 4, no. 12, pp. 1458–1462, 2009.

[44] G. Umana-Membreno, B. Klein, H. Kala et al., "Vertical minority carrier electron transport in p-type InAs/GaSb type-II superlattices," *Applied Physics Letters*, vol. 101, no. 25, Article ID 253515, 2012.

[45] P. Christol, L. Konczewicz, Y. Cuminal, H. Aït-Kaci, J. B. Rodriguez, and A. Joullié, "Electrical properties of short period InAs/GaSb superlattice," *Physica Status Solidi C*, vol. 4, no. 4, pp. 1494–1498, 2007.

[46] C. Cervera, J. B. Rodriguez, J. P. Perez et al., "Unambiguous determination of carrier concentration and mobility for InAs/GaSb superlattice photodiode optimization," *Journal of Applied Physics*, vol. 106, no. 3, Article ID 033709, 2009.

[47] H. J. Haugan, S. Elhamri, F. Szmulowicz, B. Ullrich, G. J. Brown, and W. C. Mitchel, "Study of residual background carriers in midinfrared InAsGaSb superlattices for unfcooled detector operation," *Applied Physics Letters*, vol. 92, no. 7, Article ID 071102, 2008.

[48] F. Szmulowicz, S. Elhamri, H. J. Haugan, G. J. Brown, and W. C. Mitchel, "Demonstration of interface-scattering-limited electron mobilities in InAs/GaSb superlattices," *Journal of Applied Physics*, vol. 101, no. 4, Article ID 043706, 2007.

[49] F. Szmulowicz, S. Elhamri, H. J. Haugan, G. J. Brown, and W. C. Mitchel, "Carrier mobility as a function of carrier density in type-II InAs/GaSb superlattices," *Applied Physics Letters*, vol. 105, Article ID 074303, 2009.

[50] K. Mahalingam, H. J. Haugan, G. J. Brown, and A. J. Aronow, "Strain analysis of compositionally tailored interfaces in InAs/GaSb superlattices," *Applied Physics Letters*, vol. 103, no. 21, Article ID 211605, 2013.

[51] H. Kim, Y. Meng, J. L. Rouviere, D. Isheim, D. N. Seidman, and J. M. Zuo, "Atomic resolution mapping of interfacial intermixing and segregation in InAs/GaSb superlattices: a correlative study," *Journal of Applied Physics*, vol. 113, no. 10, Article ID 103511, 2013.

[52] Z. Xu, J. Chen, F. Wang, Y. Zhou, C. Jin, and L. He, "Interface layer control and optimization of InAs/GaSb type-II superlattices grown by molecular beam epitaxy," *Journal of Crystal Growth*, vol. 386, pp. 220–225, 2014.

[53] B. Arikan, G. Korkmaz, Y. E. Suyolcu, B. Aslan, and U. Serincan, "On the structural characterization of InAs/GaSb type-II superlattices: the effect of interfaces for fixed layer thicknesses," *Thin Solid Films*, vol. 548, pp. 288–291, 2013.

[54] Y. Ashuach, Y. Kauffmann, C. Saguy et al., "Quantification of atomic intermixing in short-period InAs/GaSb superlattices for infrared photodetectors," *Journal of Applied Physics*, vol. 113, no. 18, Article ID 184305, 2013.

[55] J. Steinshnider, M. Weimer, R. Kaspi, and G. W. Turner, "Visualizing interfacial structure at non-common-atom heterojunctions with cross-sectional scanning tunneling microscopy," *Physical Review Letters*, vol. 85, no. 14, pp. 2953–2956, 2000.

[56] J. Steinshnider, J. Harper, M. Weimer, C.-H. Lin, S. S. Pei, and D. H. Chow, "Origin of antimony segregation in GaInSb/InAs strained-layer superlattices," *Physical Review Letters*, vol. 85, no. 21, pp. 4562–4565, 2000.

[57] R. Kaspi, J. Steinshnider, M. Weimer, C. Moeller, and A. Ongstad, "As-soak control of the InAs-on-GaSb interface," *Journal of Crystal Growth*, vol. 225, no. 2–4, pp. 544–549, 2001.

[58] R. Kaspi, "Compositional abruptness at the InAs-on-GaSb interface: optimizing growth by using the Sb desorption signature," *Journal of Crystal Growth*, vol. 201-202, pp. 864–867, 1999.

[59] P. M. Thibado, B. R. Bennett, M. E. Twigg, B. V. Shanabrook, and L. J. Whitman, "Origins of interfacial disorder in GaSb/InAs superlattices," *Applied Physics Letters*, vol. 67, pp. 3578–3580, 1995.

[60] E. M. Jackson, G. I. Boishin, E. H. Aifer, B. R. Bennett, and L. J. Whitman, "Arsenic cross-contamination in GaSb/InAs superlattices," *Journal of Crystal Growth*, vol. 270, no. 3-4, pp. 301–308, 2004.

[61] E. Luna, B. Satpati, J. B. Rodriguez, A. N. Baranov, E. Tourní, and A. Trampert, "Interfacial intermixing in InAs/GaSb short-period-superlattices grown by molecular beam epitaxy," *Applied Physics Letters*, vol. 96, no. 2, Article ID 021904, 2010.

[62] M. A. Kinch, "Fundamental physics of infrared detector materials," *Journal of Electronic Materials*, vol. 29, no. 6, pp. 809–817, 2000.

[63] A. Rogalski, "Third-generation infrared photon detectors," *Optical Engineering*, vol. 42, no. 12, pp. 3498–3516, 2003.

[64] A. Rogalski, "Infrared detectors: status and trends," *Progress in Quantum Electronics*, vol. 27, no. 2-3, pp. 59–210, 2003.

[65] C. Downs and T. E. Vanderveld, "Progress in infrared photodetectors since 2000," *Sensors*, vol. 13, pp. 5054–5098, 2013.

[66] M. Walther, J. Schmitz, R. Rehm et al., "Growth of InAs/GaSb short-period superlattices for high-resolution mid-wavelength infrared focal plane array detectors," *Journal of Crystal Growth*, vol. 278, no. 1–4, pp. 156–161, 2005.

[67] Y. Wei, A. Hood, H. Yau et al., "Uncooled operation of type-II InAs/GaSb superlattice photodiodes in the midwavelength infrared range," *Applied Physics Letters*, vol. 86, no. 23, Article ID 233106, pp. 1–3, 2005.

[68] E. Plis, J. B. Rodriguez, H. S. Kim et al., "Type II InAsGaSb strain layer superlattice detectors with p-on-n polarity," *Applied Physics Letters*, vol. 91, no. 13, Article ID 133512, 2007.

[69] I. Vurgaftman, E. H. Aifer, C. L. Canedy et al., "Graded band gap for dark-current suppression in long-wave infrared W-structured type-II superlattice photodiodes," *Applied Physics Letters*, vol. 89, no. 12, Article ID 121114, 2006.

[70] D. Z.-Y. Ting, C. J. Hill, A. Soibel et al., "A high-performance long wavelength superlattice complementary barrier infrared detector," *Applied Physics Letters*, vol. 95, no. 2, Article ID 023508, 2009.

[71] P. Y. Delaunay and M. Razeghi, "Spatial noise and correctability of type-II InAs/GaSb focal plane arrays," *IEEE Journal of Quantum Electronics*, vol. 46, no. 4, pp. 584–588, 2010.

[72] N. Gautam, S. Myers, A. V. Barve et al., "Barrier engineered infrared photodetectors based on type-II InAs/GaSb strained layer superlattices," *IEEE Journal of Quantum Electronics*, vol. 49, no. 2, pp. 211–217, 2013.

[73] Y. Wei, A. Gin, M. Razeghi, and G. J. Brown, "Type II InAs/GaSb superlattice photovoltaic detectors with cutoff wavelength approaching 32 μm," *Applied Physics Letters*, vol. 81, no. 19, pp. 3675–3677, 2002.

[74] A. Hood, M. Razeghi, E. H. Aifer, and G. J. Brown, "On the performance and surface passivation of type II InAs/GaSb superlattice photodiodes for the very-long-wavelength infrared," *Applied Physics Letters*, vol. 87, no. 15, Article ID 151113, pp. 1–3, 2005.

[75] S. D. Gunapala, D. Z. Ting, C. J. Hill et al., "Demonstration of a 1024×1024 Pixel InAsGaSb superlattice focal plane array," *IEEE Photonics Technology Letters*, vol. 22, no. 24, pp. 1856–1858, 2010.

[76] A. Haddadi, S. Ramezani-Darvish, G. Chen, A. M. Hoang, B.-M. Nguyen, and M. Razeghi, "High operability 1024×1024 long wavelength type-II superlattice focal plane array," *IEEE Journal of Quantum Electronics*, vol. 48, no. 2, pp. 221–228, 2012.

[77] A. M. Hoang, G. Chen, A. Haddadi, and M. Razeghi, "Demonstration of high-performance biasselectable dual-band short-mid-wavelength infrared photodetectors based on type-II InAs/GaSb/AlSb superlattices," *Applied Physics Letters*, vol. 102, Article ID 011108, 2013.

[78] R. Rehm, M. Walther, F. Rutz et al., "Dual-color InAs/GaSb superlattice focal-plane array technology," *Journal of Electronic Materials*, vol. 40, no. 8, pp. 1738–1743, 2011.

[79] A. Khoshakhlagh, J. B. Rodriguez, E. Plis et al., "Bias dependent dual band response from InAsGa (In) Sb type II strain layer superlattice detectors," *Applied Physics Letters*, vol. 91, no. 26, Article ID 263504, 2007.

[80] E. Plis, S. S. Krishna, E. P. Smith, S. Johnson, and S. Krishna, "Voltage controllable dual-band response from InAs/GaSb strained layer superlattice detectors with nBn design," *Electronics Letters*, vol. 47, no. 2, pp. 133–134, 2011.

[81] J. Huang, W. Ma, C. Cao et al., "Mid wavelength type II InAs/GaSb superlattice photodetector using SiO_xN_y passivation," *Japanese Journal of Applied Physics*, vol. 51, Article ID 074002, 2012.

[82] N. Gautam, M. Naydenkov, S. Myers et al., "Three color infrared detector using InAs/GaSb superlattices with unipolar barriers," *Applied Physics Letters*, vol. 98, no. 12, Article ID 121106, 2011.

[83] B.-M. Nguyen, D. Hoffman, P.-Y. Delaunay, and M. Razeghi, "Dark current suppression in type II InAsGaSb superlattice long wavelength infrared photodiodes with M-structure barrier," *Applied Physics Letters*, vol. 91, no. 16, Article ID 163511, 2007.

[84] E. H. Aifer, J. H. Warner, C. L. Canedy et al., "Shallow-etch mesa isolation of graded-bandgap W-structured type II superlattice photodiodes," *Journal of Electronic Materials*, vol. 39, pp. 1070–1079, 2010.

[85] O. Salihoglu, A. Muti, K. Kutluer et al., "N-structure for type-II superlattice photodetectors," *Applied Physics Letters*, vol. 101, no. 7, Article ID 073505, 2012.

[86] J. B. Rodriguez, E. Plis, G. Bishop et al., "NBn structure based on InAs/GaSb type-II strained layer superlattices," *Applied Physics Letters*, vol. 91, no. 4, Article ID 043514, 2008.

[87] H. S. Kim, E. Plis, J. B. Rodriguez et al., "Mid-IR focal plane array based on type-II InAsGaSb strain layer superlattice detector with nBn design," *Applied Physics Letters*, vol. 92, no. 18, Article ID 183502, 2008.

[88] A. Rogalski, J. Antoszewski, and L. Faraone, "Third-generation infrared photodetector arrays," *Journal of Applied Physics*, vol. 105, no. 9, Article ID 091101, 2009.

[89] A. Rogalski, "Progress in focal plane array technologies," *Progress in Quantum Electronics*, vol. 36, p. 342, 2012.

[90] M. Sundaram, A. Reisinger, R. Dennis et al., "Evolution of array format of longwave infrared Type-II SLS FPAs with high quantum efficiency," *Infrared Physics & Technology*, vol. 59, pp. 12–17, 2013.

[91] M. Razeghi, A. Haddadi, A. Hoang et al., "Advances in antimonide-based Type-II superlattices for infrared detection and imaging at center for quantum devices," *Infrared Physics & Technology*, vol. 59, pp. 41–52, 2013.

[92] D. Z. Ting, A. Soibel, S. A. Keo et al., "Development of quantum well, quantum dot, and type II superlattice infrared photodetectors," *Journal of Applied Remote Sensing*, vol. 8, Article ID 084998, 2014.

[93] D. R. Rhiger, "Performance comparison of long-wavelength infrared type II superlattice devices with HgCdTe," *Journal of Electronic Materials*, vol. 40, no. 8, pp. 1815–1822, 2011.

[94] A. Rogalski, *New Ternary Alloy Systems for Infrared Detectors*, SPIE, Bellingham, Wash, USA, 1994.

[95] S. Maimon and G. W. Wicks, "nBn detector, an infrared detector with reduced dark current and higher operating temperature," *Applied Physics Letters*, vol. 89, no. 15, Article ID 151109, 2006.

[96] W. Shockley and J. W. T. Read, "Statistics of the recombinations of holes and electrons," *Physical Review*, vol. 87, no. 5, pp. 835–842, 1952.

[97] W. Walukiewicz, "Defect reactions at metal-semiconductor and semiconductor-semiconductor interfaces," *Materials Research Society Symposium Proceedings*, vol. 148, p. 137, 1989.

[98] S. P. Svensson, D. Donetsky, D. Wang, H. Hier, F. J. Crowne, and G. Belenky, "Growth of type II strained layer superlattice, bulk InAs and GaSb materials for minority lifetime characterization," *Journal of Crystal Growth*, vol. 334, no. 1, pp. 103–107, 2011.

[99] B. C. Connelly, G. D. Metcalfe, H. Shen, and M. Wraback, "Direct minority carrier lifetime measurements and recombination mechanisms in long-wave infrared type II superlattices using time-resolved photoluminescence," *Applied Physics Letters*, vol. 97, no. 25, Article ID 251117, 2010.

[100] E. H. Steenbergen, B. C. Connelly, G. D. Metcalfe et al., "Significantly improved minority carrier lifetime observed in a long-wavelength infrared III-V type-II superlattice comprised of InAs/InAsSb," *Applied Physics Letters*, vol. 99, no. 25, Article ID 251110, 2011.

[101] G. Belenky, G. Kipshidze, D. Donetsky et al., "Effects of carrier concentration and phonon energy on carrier lifetime in Type-2 SLS and properties of $InAs_{1-X}Sb_X$ alloys," in *Infrared Technology and Applications XXXVII*, vol. 8012 of *Proceedings of SPIE*, April 2011.

[102] L. Murray, K. Lokovic, B. Olson, A. Yildirim, T. Boggess, and J. Prineas, "Effects of growth rate variations on carrier lifetime and interface structure in InAs/GaSb superlattices," *Journal of Crystal Growth*, vol. 386, pp. 194–198, 2014.

[103] Q. K. Yang, C. Pfahler, J. Schmitz, W. Pletschen, and F. Fuchs, "Trap centers and minority carrier lifetimes in InAs/(GaIn)Sb superlattice long wavelength photodetectors," in *Quantum Sensing: Evolution and Revolution from Past to Future*, vol. 4999 of *Proceedings of SPIE*, pp. 448–456, January 2003.

[104] E. C. F. Da Silva, D. Hoffman, A. Hood, B. M. Nguyen, P. Y. Delaunay, and M. Razeghi, "Influence of residual impurity background on the nonradiative recombination processes in high purity InAsGaSb superlattice photodiodes," *Applied Physics Letters*, vol. 89, no. 24, Article ID 243517, 2006.

[105] H. Mohseni, M. Razeghi, G. J. Brown, and Y. S. Park, "High-performance InAs/GaSb superlattice photodiodes for the very long wavelength infrared range," *Applied Physics Letters*, vol. 78, no. 15, pp. 2107–2109, 2001.

[106] J. V. Li, S. L. Chuang, E. M. Jackson, and E. Aifer, "Minority carrier diffusion length and lifetime for electrons in a type-II InAs/GaSb superlattice photodiode," *Applied Physics Letters*, vol. 85, no. 11, pp. 1984–1986, 2004.

[107] D. Donetsky, G. Belenky, S. Svensson, and S. Suchalkin, "Minority carrier lifetime in type-2 InAs-GaSb strained-layer superlattices and bulk HgCdTe materials," *Applied Physics Letters*, vol. 97, no. 5, Article ID 052108, 2010.

[108] B. V. Olson, E. A. Shaner, J. K. Kim et al., "Time-resolved optical measurements of minority carrier recombination in a mid-wave infrared InAsSb alloy and InAs/InAsSb superlattice," *Applied Physics Letters*, vol. 101, Article ID 092109, 2012.

[109] D. Lackner, M. Steger, M. L. W. Thewalt et al., "InAs/InAsSb strain balanced superlattices for optical detectors: material properties and energy band simulations," *Journal of Applied Physics*, vol. 111, no. 3, Article ID 034507, 2012.

[110] C. M. Ciesla, B. N. Murdin, C. R. Pidgeon et al., "Suppression of Auger recombination in arsenic-rich $InAs_{1-x}Sb_x$ strained layer super-lattices," *Journal of Applied Physics*, vol. 80, no. 5, pp. 2994–2997, 1996.

[111] T. Schuler-Sandy, S. Myers, B. Klein et al., "Gallium free type II $InAs/InAs_xSb_{1-x}$ superlattice photodetectors," *Applied Physics Letters*, vol. 101, no. 7, Article ID 071111, 2012.

[112] O. O. Cellek, Z. Y. He, Z. Y. Lin, H. S. Kim, S. Liu, and Y. H. Zhang, "InAs/InAsSb type-II superlattice infrared nBn photodetectors and their potential for operation at high temperatures," in *Quantum Sensing and Nanophotonic Devices X*, vol. 8631 of *Proceedings of SPIE*, 2013.

[113] B. V. Olson, E. A. Shaner, J. K. Kim et al., "Identification of dominant recombination mechanisms in narrow-bandgap InAs/InAsSb type-II superlattices and InAsSb alloys," *Applied Physics Letters*, vol. 103, no. 5, Article ID 052106, 2013.

[114] R. Q. Yang, Z. Tian, J. F. Klem, T. D. Mishima, M. B. Santos, and M. B. Johnson, "Interband cascade photovoltaic devices," *Applied Physics Letters*, vol. 96, no. 6, Article ID 063504, 2010.

[115] R. Q. Yang, Z. Tian, Z. Cai, J. F. Klem, M. B. Johnson, and H. C. Liu, "Interband-cascade infrared photodetectors with superlattice absorbers," *Journal of Applied Physics*, vol. 107, no. 5, Article ID 054514, 2010.

[116] A. Tian, R. T. Hinkey, R. Q. Yang et al., "Interband cascade infrared photodetectors with enhanced electron barriers and p-type superlattice absorbers," *Journal of Applied Physics*, vol. 111, no. 2, Article ID 024510, 2012.

[117] N. Gautam, S. Myers, A. V. Barve et al., "High operating temperature interband cascade midwave infrared detector based on type-II InAs/GaSb strained layer superlattice," *Applied Physics Letters*, vol. 101, no. 2, Article ID 021106, 2012.

[118] Z. B. Tian, T. Schuler-Sandy, and S. Krishna, "Electron barrier study of mid-wave infrared interband cascade photodetectors," *Applied Physics Letters*, vol. 103, Article ID 083601, 2013.

[119] K. Banerjee, S. Ghosh, S. Mallick, E. Plis, S. Krishna, and C. Grein, "Midwave infrared InAs/GaSb strained layer superlattice hole avalanche photodiode," *Applied Physics Letters*, vol. 94, no. 20, Article ID 201107, 2009.

[120] S. Mallick, K. Banerjee, S. Ghosh, J. B. Rodriguez, and S. Krishna, "Midwavelength infrared avalanche photodiode using InAs-GaSb strain layer superlattice," *IEEE Photonics Technology Letters*, vol. 19, no. 22, pp. 1843–1845, 2007.

[121] S. Mallick, K. Banerjee, S. Ghosh et al., "Ultralow noise midwave infrared InAs-GaSb strain layer superlattice avalanche photodiode," *Applied Physics Letters*, vol. 91, no. 24, Article ID 241111, 2007.

[122] A. P. Ongstad, R. Kaspi, C. E. Moeller et al., "Spectral blueshift and improved luminescent properties with increasing GaSb layer thickness in InAs-GaSb type-II superlattices," *Journal of Applied Physics*, vol. 89, no. 4, pp. 2185–2188, 2001.

[123] P.-Y. Delaunay, A. Hood, B. M. Nguyen, D. Hoffman, Y. Wei, and M. Razeghi, "Passivation of type-II InAsGaSb double heterostructure," *Applied Physics Letters*, vol. 91, no. 9, Article ID 091112, 2007.

[124] E. Plis, M. N. Kutty, and S. Krishna, "Passivation techniques for InAs/GaSb strained layer superlattice detectors," *Laser & Photonics Reviews*, vol. 7, pp. 1–15, 2012.

[125] F. M. Mohammedy and M. J. Deen, "Growth and fabrication issues of GaSb-based detectors," *Journal of Materials Science: Materials in Electronics*, vol. 20, no. 11, pp. 1039–1058, 2009.

[126] G. J. Brown, "Type-II InAs/GaInSb superlattices for infrared detection: an overview," in *Infrared Technology and Applications XXXI*, vol. 5783 of *Proceedings of SPIE*, pp. 65–77, April 2005.

[127] K. Banerjee, S. Ghosh, E. Plis, and S. Krishna, "Study of short-and long-term effectiveness of ammonium sulfide as surface passivation for InAs/GaSb superlattices using X-ray photoelectron spectroscopy," *Journal of Electronic Materials*, vol. 39, no. 10, pp. 2210–2214, 2010.

[128] T. Wada and N. Kitamura, "X-Ray photoelectron spectra of an electron-beam oxide layer on GaSb," *Japanese Journal of Applied Physics*, vol. 27, no. 4, pp. 686–687, 1988.

[129] E. Plis, M. N. Kutty, S. Myers et al., "Passivation of long-wave infrared InAs/GaSb strained layer superlattice detectors," *Infrared Physics and Technology*, vol. 54, no. 3, pp. 252–257, 2011.

[130] A. Gin, Y. Wei, J. Bae, A. Hood, J. Nah, and M. Razeghi, "Passivation of type II InAs/GaSb superlattice photodiodes," *Thin Solid Films*, vol. 447-448, pp. 489–492, 2004.

[131] E. K. Huang, B.-M. Nguyen, D. Hoffman, P.-Y. Delaunay, and M. Razeghi, "Inductively coupled plasma etching and processing techniques for type-II InAs/GaSb superlattices infrared detectors toward high fill factor focal plane arrays," in *Quantum Sensing and Nanophotonic Devices VI*, vol. 7222 of *Proceedings of SPIE*, January 2009.

[132] E. K.-W. Huang, D. Hoffman, B.-M. Nguyen, P.-Y. Delaunay, and M. Razeghi, "Surface leakage reduction in narrow band gap type-II antimonide-based superlattice photodiodes," *Applied Physics Letters*, vol. 94, no. 5, Article ID 053506, 2009.

[133] R. Rehm, M. Walther, F. Fuchs, J. Schmitz, and J. Fleissner, "Passivation of InAs/(GaIn) Sb short-period superlattice photodiodes with 10 μm cutoff wavelength by epitaxial overgrowth with $Al_xGa_{1-x}As_ySb_{1-y}$," *Applied Physics Letters*, vol. 86, no. 17, Article ID 173501, pp. 1–3, 2005.

[134] B.-M. Nguyen, D. Hoffman, E. K.-W. Huang, P.-Y. Delaunay, and M. Razeghi, "Background limited long wavelength infrared type-II InAs/GaSb superlattice photodiodes operating at 110 K," *Applied Physics Letters*, vol. 93, no. 12, Article ID 123502, 2008.

[135] R. Chaghi, C. Cervera, H. Aït-Kaci, P. Grech, J. B. Rodriguez, and P. Christol, "Wet etching and chemical polishing of InAs/GaSb superlattice photodiodes," *Semiconductor Science and Technology*, vol. 24, no. 6, Article ID 065010, 2009.

[136] C. Cervera, J. B. Rodriguez, R. Chaghi, H. At-Kaci, and P. Christol, "Characterization of midwave infrared InAs/GaSb superlattice photodiode," *Journal of Applied Physics*, vol. 106, no. 2, Article ID 024501, 2009.

[137] Y. Chen, A. Moy, S. Xin, K. Mi, and P. P. Chow, "Improvement of R0A product of type-II InAs/GaSb superlattice MWIR/LWIR photodiodes," *Infrared Physics and Technology*, vol. 52, no. 6, pp. 340–343, 2009.

[138] S. dip Das, S. L. Tan, S. Zhang, Y. L. Goh, C. H. Ting, and J. David, "Development of LWIR photodiodes based on InAs/GaSb type-II strained layer superlattices," in *Proceedings of the 6th EMRS DTC Technical Conference*, vol. B7, Edinburgh, UK, 2009.

[139] M. N. Kutty, E. Plis, A. Khoshakhlagh et al., "Study of surface treatments on InAs/GaSb superlattice lwir detectors," *Journal of Electronic Materials*, vol. 39, no. 10, pp. 2203–2209, 2010.

[140] M. Sundaram, A. Reisinger, R. Dennis et al., "Longwave infrared focal plane arrays from type-II strained layer superlattices," *Infrared Physics and Technology*, vol. 54, no. 3, pp. 243–246, 2011.

[141] Y. T. Kim, D. S. Kim, and D. H. Yoon, "PECVD SiO_2 and SiON films dependant on the rf bias power for low-loss silica waveguide," *Thin Solid Films*, vol. 475, no. 1-2, pp. 271–274, 2005.

[142] J. A. Nolde, R. Stine, E. M. Jackson et al., "Effect of the oxide-semiconductor interface on the passivation of hybrid type-II superlattice long-wave infrared photodiodes," in *Quantum Sensing and Nanophotonic Devices VIII*, vol. 7945 of *Proceedings of SPIE*, January 2011.

[143] G. Chen, B.-M. Nguyen, A. M. Hoang, E. K. Huang, S. R. Darvish, and M. Razeghi, "Elimination of surface leakage in gate controlled type-II InAs/GaSb mid-infrared photodetectors," *Applied Physics Letters*, vol. 99, no. 18, Article ID 183503, 2011.

[144] T. Tansel, K. Kutluer, Ö. Salihoglu et al., "Effect of the passivation layer on the noise characteristics of mid-wave-infrared InAs/GaSb superlattice photodiodes," *IEEE Photonics Technology Letters*, vol. 24, no. 9, pp. 790–792, 2012.

[145] A. Hood, P.-Y. Delaunay, D. Hoffman et al., "Near bulk-limited R0A of long-wavelength infrared type-II InAs/GaSb superlattice photodiodes with polyimide surface passivation," *Applied Physics Letters*, vol. 90, no. 23, Article ID 233513, 2007.

[146] H. S. Kim, E. Plis, A. Khoshakhlagh et al., "Performance improvement of InAs/GaSb strained layer superlattice detectors by reducing surface leakage currents with SU-8 passivation," *Applied Physics Letters*, vol. 96, no. 3, Article ID 033502, 2010.

[147] E. A. DeCuir Jr., J. W. Little, and N. Baril, "Addressing surface leakage in type-II InAs/GaSb superlattice materials using novel approaches to surface passivation," in *Infrared Sensors, Devices, and Applications; and Single Photon Imaging II*, vol. 8155 of *Proceedings of SPIE*, August 2011.

[148] H. S. Kim, E. Plis, N. Gautam et al., "Reduction of surface leakage current in InAs/GaSb strained layer long wavelength superlattice detectors using SU-8 passivation," *Applied Physics Letters*, vol. 97, no. 14, Article ID 143512, 2010.

[149] D. Sanchez, L. Cerutti, and E. Tournie, "Selective lateral etching of InAs/GaSb tunnel junctions for mid-infrared photonics," *Semiconductor Science and Technology*, vol. 27, no. 8, Article ID 085011, 2012.

[150] G. A. Umana-Membreno, H. Kalaa, B. Klein et al., "Electronic transport in InAs/GaSb type-II superlattices for long wavelength infrared focal plane array applications," in *Infrared Technology and Applications XXXVIII*, vol. 8353 of *Proceedings of SPIE*, May 2012.

[151] C. J. Sandroff, M. S. Hegde, and C. C. Chang, "Structure and stability of passivating arsenic sulfide phases on GaAs surfaces," *Journal of Vacuum Science & Technology B: Microelectronics and Nanometer Structures*, vol. 7, pp. 841–844, 1989.

[152] C. J. Spindt, D. Liu, K. Miyano et al., "Vacuum ultraviolet photoelectron spectroscopy of $(NH_4)_2S$-treated GaAs (100) surfaces," *Applied Physics Letters*, vol. 55, no. 9, pp. 861–863, 1989.

[153] V. N. Bessolov, E. V. Konenkova, and M. V. Lebedev, "Sulfidization of GaAs in alcoholic solutions: a method having an impact on efficiency and stability of passivation," *Materials Science and Engineering B*, vol. 44, no. 1–3, pp. 376–379, 1997.

[154] H. Oigawa, J.-F. Fan, Y. Nannichi, H. Sugahara, and M. Oshima, "Universal passivation effect of $(NH_4)_2S_x$ treatment on the surface of III-V compound semiconductors," *Japanese Journal of Applied Physics*, vol. 30, no. 3, pp. 322–325, 1991.

[155] D. Y. Petrovykh, M. J. Yang, and L. J. Whitman, "Chemical and electronic properties of sulfur-passivated InAs surfaces," *Surface Science*, vol. 523, no. 3, pp. 231–240, 2003.

[156] M. Pérotin, P. Coudray, L. Gouskov et al., "Passivation of GaSb by sulfur treatment," *Journal of Electronic Materials*, vol. 23, no. 1, pp. 7–12, 1994.

[157] P. S. Dutta, K. S. Sangunni, H. L. Bhat, and V. Kumar, "Sulphur passivation of gallium antimonide surfaces," *Applied Physics Letters*, vol. 65, no. 13, pp. 1695–1697, 1994.

[158] S. Basu and P. Barman, "Chemical modification and characterization of Te-doped n-GaSb (111) single crystals for device application," *Journal of Vacuum Science & Technology B: Microelectronics and Nanometer Structures*, vol. 10, no. 3, pp. 1078–1080, 1992.

[159] V. N. Bessolov, M. V. Lebedev, E. B. Novikov, and B. V. Tsarenkov, "Sulfide passivation of III-V semiconductors: kinetics of the photoelectrochemical reaction," *Journal of Vacuum Science & Technology B: Microelectronics and Nanometer Structures*, vol. 11, pp. 10–14, 1993.

[160] V. N. Bessolov, Y. V. Zhilyaev, E. V. Konenkova, and M. V. Lebedev, "Sulfide passivation of III-V semiconductor surfaces: role of the sulfur ionic charge and of the reaction potential of the solution," *Journal of Technical Physics*, vol. 43, no. 8, pp. 983–985, 1998.

[161] T. Ohno, "Passivation of GaAs(001) surfaces by chalcogen atoms (S, Se and Te)," *Surface Science*, vol. 255, no. 3, pp. 229–236, 1991.

[162] T. Ohno and K. Shiraishi, "First-principles study of sulfur passivation of GaAs(001) surfaces," *Physical Review B*, vol. 42, no. 17, pp. 11194–11197, 1990.

[163] A. Gin, Y. Wei, A. Hood et al., "Ammonium sulfide passivation of Type-II InAs/GaSb superlattice photodiodes," *Applied Physics Letters*, vol. 84, no. 12, pp. 2037–2039, 2004.

[164] K. Banerjee, J. Huang, S. Ghosh et al., "Surface study of thioacetamide and zinc sulfide passivated long wavelength infrared type-II strained layer superlattice," in *Infrared Technology and Applications XXXVII*, vol. 8012 of *Proceedings of SPIE*, April 2011.

[165] E. Plis, J.-B. Rodriguez, S. J. Lee, and S. Krishna, "Electrochemical sulphur passivation of InAs/GaSb strain layer superlattice detectors," *Electronics Letters*, vol. 42, no. 21, pp. 1248–1249, 2006.

[166] R. Xu and C. G. Takoudis, "Chemical passivation of GaSb-based surfaces by atomic layer deposited ZnS using diethylzinc and hydrogen sulfide," *Journal of Vacuum Science and Technology A: Vacuum, Surfaces and Films*, vol. 30, no. 1, Article ID 01A145, 2012.

[167] L. Zhang, L. X. Zhang, X. W. Shen et al., "Research on passivation of type II InAs/GaSb superlattice photodiodes," in *International Symposium on Photoelectronic Detection and Imaging 2013: Infrared Imaging and Applications*, vol. 890731 of *Proceedings of SPIE*, 2013.

[168] S. C. Lee, E. Plis, S. Krishna, and S. R. J. Brueck, "Mid-infrared transmission enhancement through sub-wavelength metal hole array using impedance-matching dielectric layer," *Electronics Letters*, vol. 45, no. 12, pp. 643–645, 2009.

[169] M. Zamiri, E. Plis, J. O. Kim et al., "MWIR superlattice detectors integrated with back side illuminated plasmonic coupler," Unpablished.

[170] F. Szmulowicz and G. J. Brown, "GaSb for passivating type-II InAs/GaSb superlattice mesas," *Infrared Physics and Technology*, vol. 53, no. 5, pp. 305–307, 2010.

[171] E. Plis, B. Klein, S. Myers et al., "Type-II InAs/GaSb strained layer superlattices grown on GaSb (111)B substrate," *Journal of Vacuum Science and Technology B*, vol. 31, no. 1, 2013.

[172] F. Szmulowicz, H. J. Haugan, and G. J. Brown, "Proposal for (110) InAs/GaSb superlattices for infrared detection," in *Quantum Sensing and Nanophotonic Devices V*, vol. 6900 of *Proceedings of SPIE*, January 2008.

[173] C. Zhou, B. M. Nguyen, M. Razeghi, and M. Grayson, "Thermal conductivity of InAs/GaSb type-II superlattice," *Journal of Electronic Materials*, vol. 41, pp. 2322–2325, 2012.

[174] V. V. R. Kishore, B. Partoens, and F. M. Peeters, "Electronic structure of InAs/GaSb core-shell nanowires," *Physical Review B*, vol. 86, Article ID 165439, 2012.

[175] B. Ganjipour, M. Ek, B. M. Borg et al., "Carrier control and transport modulation in GaSb/InAsSb core/shell nanowires," *Applied Physics Letters*, vol. 101, no. 10, Article ID 103501, 2012.

[176] R. Li, Y. Lu, S. D. Chae et al., "InAs/AlGaSb heterojunction tunnel field-effect transistor with tunnelling in-line with the gate field," *Physica Status Solidi C*, vol. 9, no. 2, pp. 389–392, 2012.

[177] W. Pan, J. F. Klem, J. K. Kim, M. Thalakulam, M. J. Cich, and S. K. Lyo, "Chaotic quantum transport near the charge neutrality point in inverted type-II InAs/GaSb field-effect transistors," *Applied Physics Letters*, vol. 102, no. 3, Article ID 033504, 2013.

[178] H. Lotfi, R. T. Hinkey, L. Li, R. Q. Yang, J. F. Klem, and M. B. Johnson, "Narrow-bandgap photovoltaic devices operating at room temperature and above with high open-circuit voltage," *Applied Physics Letters*, vol. 102, no. 21, Article ID 211103, 2013.

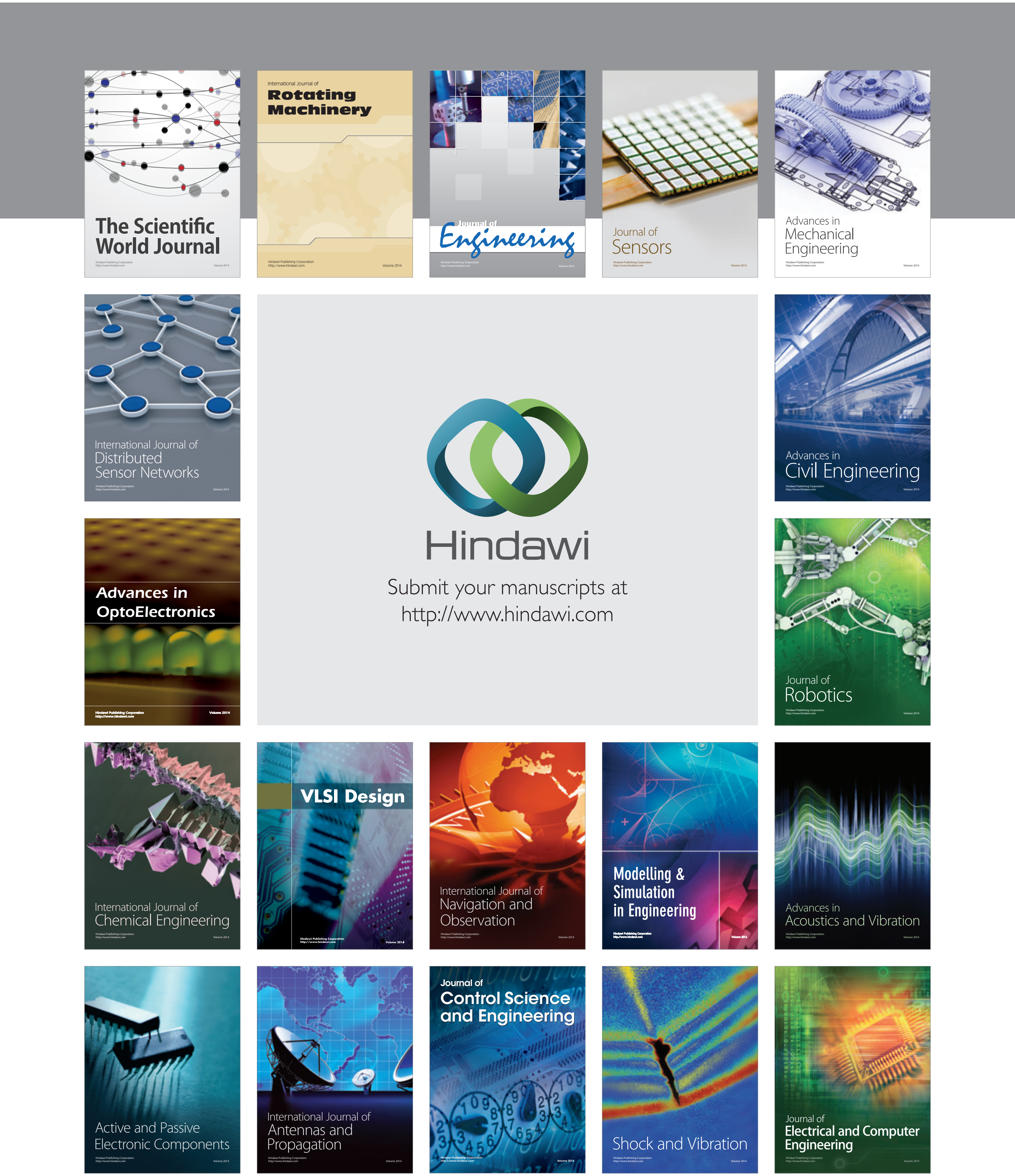
The Scientific World Journal
International Journal of Rotating Machinery
Journal of Engineering
Journal of Sensors
Advances in Mechanical Engineering
International Journal of Distributed Sensor Networks
Hindawi
Submit your manuscripts at
http://www.hindawi.com
Advances in Civil Engineering
Advances in OptoElectronics
Journal of Robotics
International Journal of Chemical Engineering
VLSI Design
International Journal of Navigation and Observation
Modelling & Simulation in Engineering
Advances in Acoustics and Vibration
Active and Passive Electronic Components
International Journal of Antennas and Propagation
Journal of Control Science and Engineering
Shock and Vibration
Journal of Electrical and Computer Engineering